

Enhanced Killing of Melanoma Cells by Simultaneously Targeting Mcl-1 and NOXA

Jian-Zhong Qin, Hong Xin, Leonid A. Sitailo, Mitchell F. Denning, and Brian J. Nickoloff

Department of Pathology, Loyola University Medical Center, Maywood, Illinois

Abstract

By deciphering the dysregulation of apoptosis in melanoma cells, new treatment approaches exploiting aberrant control mechanisms regulating cell death can be envisioned. Among the Bcl-2 family, a BH3-only member, NOXA, functions in a specific mitochondrial-based cell death pathway when melanoma cells are exposed to a proteasome inhibitor (e.g., bortezomib). Some therapeutic agents, such as bortezomib, not only induce proapoptotic Bcl-2 family members and active conformational changes in Bak and Bax but also are associated with undesirable effects, including accumulation of antiapoptotic proteins, such as Mcl-1. To enhance the bortezomib-mediated killing of melanoma cells, the apoptotic pathway involving NOXA was further investigated, leading to identification of an important target (i.e., the labile Bcl-2 homologue Mcl-1 but not other survival proteins). To reduce Mcl-1 levels, melanoma cells were pretreated with several different agents, including Mcl-1 small interfering RNA (siRNA), UV light, or the purine nucleoside analogue fludarabine. By simultaneously triggering production of NOXA (using bortezomib) as well as reducing Mcl-1 levels (using siRNA, UV light, or fludarabine), significantly enhanced killing of melanoma cells was achieved. These results show binding interactions between distinct Bcl-2 family members, such as NOXA and Mcl-1, in melanoma cells, paving the way for novel and rational therapeutic combination strategies, which target guardians of the proapoptotic Bak- and Bax-mediated pathways, against this highly aggressive and often fatal malignancy. (Cancer Res 2006; 66(19): 9636-45)

Introduction

Not only is the lifetime risk of developing melanoma increasing steadily (~1 in 75), but also in metastatic melanoma patients the average survival rate is only 6 to 10 months (1, 2). The treatment of metastatic melanoma is frequently futile because of the aggressive growth and apoptotic resistance of the tumor to various therapeutic regimens (3). The resistance of melanoma to existing treatments is linked to the large number of survival pathways and inactivation of death pathways (2). The treatment approaches that have been investigated in numerous phase III clinical trials include immunotherapy with or without dendritic cells, cytokine-based therapy, radiation therapy, and chemotherapy (4–6). Even the use of combinations of chemotherapeutic agents has not significantly

changed the overall survival benefit in any randomized clinical trials for the past 20 years. One of the primary obstacles to progress has been the lack of precise mechanistic insights by which conventional therapeutic agents either succeed or fail in killing various tumor cell types. Added to this issue has been the growing number of survival factors defined in melanoma cells that seem to present a daunting challenge for investigators attempting to overcome the apoptotic resistance of melanoma cells (7). These survival factors include members of the Bcl-2 family, such as Bcl-2 and Bcl-x_L, as well as elevated levels of survivin and Mcl-1 (8–10). Recently, we and others have successfully overcome the apoptotic resistance of melanoma cells using proteasome inhibitors (11–13), and this study extends our efforts to optimize the effectiveness of this class of antineoplastic reagents (14).

To probe into the molecular black box of melanoma cells regarding apoptosis and drug resistance (7, 8, 15), we sought to define the molecular mechanism by which a proteasome inhibitor [e.g., bortezomib (PS-341; Velcade)] can overcome the well-known apoptotic resistance of melanoma cells. Defining this pathway led to an important role for the BH3-only protein, NOXA, in the successful apoptotic response both *in vitro* and in animal-based xenograft tumor models (11–13). The induction of NOXA was found to be independent of the p53 status of the treated cells and included a transcriptional component (11–13). Because a recent phase II clinical trial using bortezomib as a single agent revealed minimal efficacy, we decided to identify molecular targets for NOXA with the perspective of using this new insight for designing a rational approach for combination therapy rather than relying on purely empirical approaches for future clinical trials (16–18).

A growing body of evidence highlights the molecular machinery involving the intrinsic or mitochondrial-based apoptotic pathway (19, 20). The overall integrity of mitochondrial function is controlled by the Bcl-2 family of proteins that include both antiapoptotic and proapoptotic members (21). These family members belong to three different classes of proteins based on their Bcl-2 homology domains, which include multidomain antiapoptotic proteins (Bcl-2, Bcl-x_L, Mcl-1, Bcl-w, and A1), multidomain proapoptotic proteins (Bak and Bax), and BH3-only proapoptotic proteins (Bid, Bad, Bim, PUMA, NOXA, and Bik). The proapoptotic BH3-only proteins, such as NOXA, are the most apical regulators of death signaling cascades and hence have become intensely studied in a variety of normal and malignant cell types (22). A recent elegant model has been proposed in which the overall apoptotic response of cells can be defined around the proapoptotic Bak and Bax family members (23–25).

According to this model, the activation of multidomain proapoptotic proteins, such as Bak and Bax, mediating toxicity is required for cell death and is normally blocked in healthy cells by the copresence of Mcl-1 and Bcl-x_L. Thus, Mcl-1 and Bcl-x_L serve as complimentary guardians to protect against cell death by binding to Bak and Bax and hence preventing their conformational state to be converted from an inactive to active or toxic status. However,

Note: J-Z. Qin and H. Xin contributed equally to this work.

Requests for reprints: Brian J. Nickoloff, Oncology Institute, Cardinal Bernardin Cancer Center, Loyola University Medical Center, Building 112, Room 301, 2160 South First Avenue, Maywood, IL 60153. Phone: 708-327-3241; Fax: 708-327-3239; E-mail: bnickol@lumc.edu.

©2006 American Association for Cancer Research.
doi:10.1158/0008-5472.CAN-06-0747

when NOXA is induced, it can displace Mcl-1 leading to the ubiquitination and proteasome-mediated degradation of Mcl-1; when Bad is present, it can displace Bcl-x_L, thereby allowing Bak and Bax to oligomerize, and in this activated conformation, Bak and Bax can mediate toxic reactions in the mitochondria culminating in cell death. Thus, a combination of both NOXA and Bad are postulated to be required to trigger cell death following a cytotoxic stimulus, although the relative contribution of the complementary guardians of Bak and Bax (e.g., Mcl-1 and Bcl-x_L) has not been defined in melanoma cells. In addition, the relative roles for activated Bak and Bax in the bortezomib-mediated cell death of melanoma cells has not been delineated. In other cell types, the relative roles for activated Bak and/or Bax have been found to be dependent on the stimulus (25–28).

Because we observed previously that inhibition of proteasome function served as a cytotoxic stimulus in melanoma cells but not in normal melanocytes, which resulted from differential induction of NOXA, the binding partner for NOXA was sought in melanoma cells and identified as Mcl-1. Once we established NOXA targeted counteracting Mcl-1 in bortezomib-treated melanoma cells, coupled with accumulation of Mcl-1 by proteasome inhibitors, agents that could be used to pretreat melanoma cells were identified to reduce Mcl-1 levels, thereby enhancing the effectiveness of bortezomib to augment the extent of NOXA-mediated cell death. Agents selected to reduce Mcl-1 levels included a genetic approach [e.g., small interfering RNA (siRNA) knockdown], a physical agent (e.g., low-dose UV light; ref. 29), and a pharmacologic agent (e.g., purine nucleoside analogue, fludarabine). Previous studies have revealed the transcriptional and translational control of Mcl-1 is characterized by a short half-life at the mRNA and protein levels (29, 30). Thus, the agents selected share the ability to disrupt both transcriptional and/or translational events and hence can reduce Mcl-1 levels (31). We were particularly interested in a purine nucleoside analogue (e.g., fludarabine) because it can inhibit both DNA and RNA synthesis and has been successfully combined in a clinical setting with other promising agents, including bortezomib, to achieve enhanced results (31–33). Although activated conformation of both Bak and Bax could be detected, the relative kinetics and extent of activation was different with higher levels of activated Bax compared with Bak in bortezomib-treated melanoma cells.

As all melanoma cell lines examined constitutively expressed Bad as well as Bak and Bax, the current results support future clinical trials for melanoma patients in which bortezomib is used to induce NOXA, combined together with an agent, such as fludarabine, which can reduce Mcl-1 levels. Such new strategies targeting mitochondria (34) exploit the specificity of BH3-only proteins and requirement for coordinated inactivation of distinct survival factors that culminate in selective killing of melanoma cells while sparing normal melanocytes. It is essential for rational design of drug combinations to better understand the genetic and molecular basis for aberrant apoptosis control in melanoma cells (16, 22), and the current results provide insight into specific therapeutic opportunities requiring bench to bedside translational studies.

Materials and Methods

Cell culture. A late-passage (>60 passages) human cutaneous melanoma cell line (C8161; mutant p53 allele) and low-passage (<20 passages) pulmonary metastatic melanoma cells (RJ002L; wild-type p53 allele) were maintained in RPMI 1640 supplemented with 10% fetal bovine serum as described previously (12). Removal of the metastatic melanoma lesion was done after patient informed consent as part of a phase I Food and Drug

Administration-approved clinical trial and approval of the Loyola Institutional Review Board.

Chemical reagents and antibodies. Bortezomib (pyrazylcarbonyl-Phe-Leu-boronate), manufactured by Millenium Pharmaceuticals (Cambridge, MA), was obtained from the Loyola University Medical Center pharmacy. Fludarabine was purchased from Sigma Chemical Co. (St. Louis, MO), and a 10 mmol/L stock solution was prepared in DMSO. Antibodies used in this study were obtained as follows: NOXA and activated Bak (35) were from Oncogene Research Products (La Jolla, CA) and Mcl-1, Bcl-2, Bcl-x_L, Bad, and poly(ADP-ribose) polymerase (PARP) were from Santa Cruz Biotechnology, Inc. (Santa Cruz, CA). Antibody to detect activated Bax from BD PharmMingen, Inc. (San Diego, CA; ref. 36). Antibody against β -actin (ICN, Irvine, CA) served as loading control.

Cell death detection. Cell viability was assessed using Apo Target Annexin V-FITC staining kits (Biosource, Camarillo, CA) according to the manufacturer's instructions. The relative percentage of cells undergoing apoptosis was quantified by flow cytometric analysis using FACSCalibur (Becton Dickinson, Palo Alto, CA) as described previously (13).

Mcl-1 retroviral constructs and infection. The Mcl-1 cDNA (kindly provided by Dr. W. Douglas Cress, University of South Florida College of Medicine) was subcloned into the *Bam*HI and *Not*I of LZRS-based retroviral expression vector. The Phoenix-Ampo retroviral packaging cells were transfected with calcium precipitation method and viral supernatants were prepared as described previously (30). RJ002L melanoma cells were seeded in six-well plates and infected with viral supernatants containing either control vector (Linker) or Mcl-1 cDNA and then were subjected to 1 μ mol/L bortezomib treatment for 24 hours.

Mcl-1 siRNA transfection. Smart pools of Mcl-1 siRNA duplexes and scrambled control duplexes were purchased from Dharmacon Research, Inc. (Lafayette, CO). C8161 melanoma cells were plated in six-well plates at a density of 15×10^4 per well, and transfection was accomplished using Oligofectamine (Invitrogen, Carlsbad, CA) in Opti-MEM following the manufacturer's protocol. After 48 hours, transfected cells were treated with bortezomib for another 24 hours.

UV light exposure. To reduce Mcl-1 levels using UV light, melanoma cells were grown in 10-cm tissue culture plates and the lid and medium were removed followed by UV irradiation using a Panelite unit (Ultralite Enterprise, Inc., Lawrenceville, GA). This light source consists of four UVB bulbs (FS36T12/UVB-VHO) and the output wavelengths of the bulbs are 65% UVB, 34% UVA, and 1% UVC as described previously (37). The UV dose was monitored with an International Light, Inc. (Newburyport, CT) radiometer fitted with a UVB detector. After irradiation, the medium was readded and the lid was replaced onto the Petri dish.

Western blot analysis. Whole-cell extracts were prepared as described previously (13). Briefly, cells were harvested by scraping monolayers and washed with PBS. Cell pellets were resuspended in CHAPS containing a protease inhibitor cocktail. Extracts were vigorously shaken at 4°C for 15 minutes followed by centrifugation. Supernatants were collected and protein concentration determined using Bradford reagent (Bio-Rad Laboratories, Hercules, CA). Protein samples (30 μ g) were resolved by SDS-PAGE and transferred to polyvinylidene difluoride membrane by electroblotting. Membranes were probed with various primary antibodies overnight at 4°C and washed, and fluorescence-labeled secondary antibody was added. After 1 hour, membranes were washed and detected with LI-COR image analysis system.

Detection of intracellular levels of activated multidomain proapoptotic proteins. Melanoma cells were fixed with 2% paraformaldehyde (10 minutes, room temperature), washed, and incubated with primary antibodies that detect the activated configuration of Bak and activated Bax diluted in fluorescence-activated cell sorting (FACS) buffer supplemented with 0.3% saponin as described previously (35, 36). Cells were then washed and incubated with FITC-labeled secondary antibody to detect levels of Bak and Bax in their activated configuration using FACS analysis. The percentage of melanoma cells containing activated Bak or Bax was assessed based on fluorescence intensity beyond the control antibody baseline levels (expressed in each figure as a relative percentage under a horizontal bracket, indicating the fluorescence intensity set points).

Immunoprecipitation. Cells treated with or without bortezomib were lysed in >10 volume of lysis buffer [50 mmol/L Tris-HCl (pH 7.4), 1% NP40, 0.25% sodium deoxycholate, 150 mmol/L NaCl, 1 mmol/L EDTA, freshly added 1 mmol/L phenylmethylsulfonyl fluoride, 1 mmol/L Na₃VO₄, 1 mmol/L NaF, protease inhibitor cocktail]. Lysate (500 µg) from each sample was precleared with protein A/G-plus agarose (Santa Cruz Biotechnology) and incubated with 2 µg of either Mcl-1 or NOXA (Zymed, San Francisco, CA) antibodies or control rabbit IgG (Santa Cruz Biotechnology) for 4 hours followed by rotating with agarose beads overnight at 4°C. After extensive washes with lysis buffer and PBS, bound proteins were eluted with sample buffer and processed for Western blotting.

Immunofluorescence staining. C8161 melanoma cells were seeded on coverslips in six-well plates, transfected with 100 nmol/L Mcl-1 siRNA or control RNA for 48 hours, and then treated with the 1 µmol/L bortezomib for 6 hours. Before finishing the treatment, the cells were labeled with 50 nmol/L MitoTracker Red CMXRos (Molecular Probes, Eugene, OR) for 30 minutes. The cells were washed with PBS and fixed with 2% paraformaldehyde (20 minutes at room temperature), permeabilized with 0.2% Triton X-100 for 10 minutes, blocked with 2% bovine serum albumin (BSA) for 30 minutes, and then stained with 1 µg/mL antibody against activated Bax (BD Transduction Laboratories, San Diego, CA) in 2% BSA for 1 hour at room temperature. After an extensive wash, cells were further incubated with goat anti-mouse IgG (Alexa Fluor 488, Molecular Probes) at 1:400 dilution for 1 hour. Before mounting, cells were stained with Hoechst 33342 at 10 µg/mL for 5 minutes. Stained cells were visualized by Zeiss microscope, Oberkochen, Germany and the images were captured with Sensys camera (run by Macprobe version 4.1 software).

Bax cross-link assay. C8161 melanoma cells were treated with either 5 mJ/cm² UV light, 1 µmol/L bortezomib alone, or 6-hour UV light pretreatment plus bortezomib. The cells were collected by brief trypsinization, washed with PBS, and suspended in 250 µL PBS. Proteins were cross-linked with 0.5% formaldehyde with shaking at room temperature for 1 hour as described (38). Cross-linking was quenched by adding 2 volumes of 2% glycine. The cells were spun, washed with PBS, and suspended in isotonic sucrose buffer. Whole-cell lysates were prepared and subjected to Western blot analysis with anti-Bax NT (Upstate, Lake Placid, NY).

Statistical analysis. The mean and SE were derived from at least three independent experiments and assessed by Student's *t* test. Results were considered significant when *P* < 0.05.

Results

Association between NOXA and Mcl-1 in bortezomib-treated melanoma cells. To determine if there were any molecular

interactions between NOXA and Mcl-1, immunoprecipitations followed by Western blot analyses were done using melanoma cells before and after bortezomib exposure (1 µmol/L; 24 hours). When whole-cell lysates were immunoprecipitated for Mcl-1, the immunoblots of C8161 melanoma cells after bortezomib exposure revealed an association between Mcl-1 and NOXA (Fig. 1, *left*). Conversely, when bortezomib-treated melanoma cells were immunoprecipitated for NOXA, the immunoblot confirmed an association between NOXA and Mcl-1 (Fig. 1, *right*). Based on these coimmunoprecipitation and Western blot studies, a physical interaction between Mcl-1 and NOXA was identified in bortezomib-treated melanoma cells.

Overexpression of Mcl-1 reduces bortezomib-induced melanoma cell apoptosis. To determine if a binding partner of NOXA, which was determined to be Mcl-1 (Fig. 1), was influencing apoptotic susceptibility, retroviral-mediated infection to overexpress Mcl-1 in melanoma cells was followed by bortezomib exposure (1 µmol/L; 24 hours). RJ002L melanoma cells are more sensitive than C8161 melanoma cells to bortezomib-induced apoptosis (13); therefore, the ability of overexpression of Mcl-1 to protect against bortezomib-induced apoptosis was studied using RJ002L cells. After confirming an ~2-fold level of overexpression of Mcl-1 (Fig. 2A), RJ002L melanoma cells were examined before and after bortezomib treatment and analyzed for extent of cell death. In control (Linker) infected melanoma cells, exposure to bortezomib increased cell death from 12% to >50% (Fig. 2B). Compared with control (Linker) infected melanoma cells, the melanoma cells overexpressing Mcl-1 were significantly less susceptible to bortezomib-induced apoptosis as the Mcl-1-overexpressing melanoma cell death response following bortezomib was 30% (Fig. 2B). In the next series of experiments, the effect of knocking down Mcl-1 levels was determined following bortezomib exposure accompanied by a more detailed biochemical dissection of molecular pathways involved in the apoptotic response.

Knockdown of Mcl-1 by siRNA enhances bortezomib-induced cell death of melanoma cells, including activation of Bak and Bax. By using a specific siRNA to knockdown Mcl-1 levels but not other Bcl-2 family members, such as Bcl-2 or Bcl-x_L, the apoptotic dependence on Mcl-1 levels could be assessed in C8161

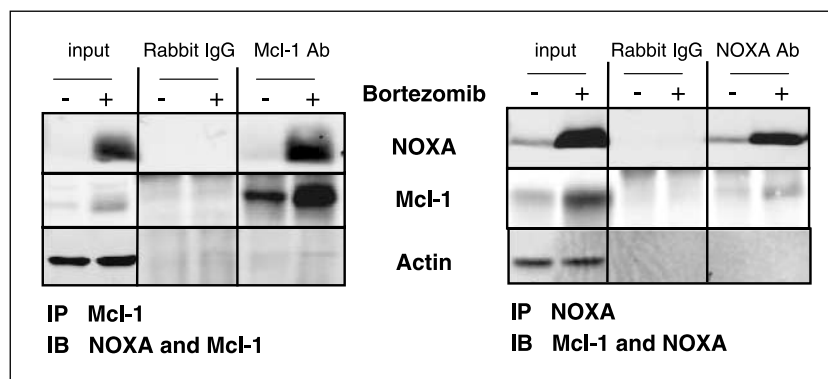
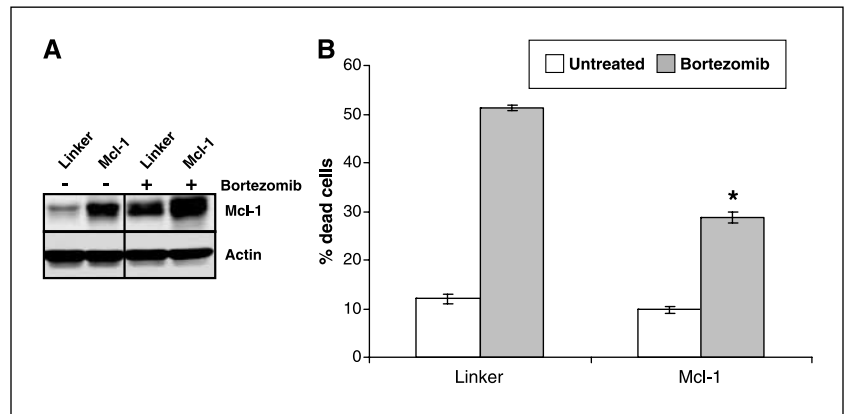


Figure 1. Binding between Mcl-1 and NOXA in bortezomib-treated C8161 melanoma cells (1 µmol/L; 24 hours). Immunoprecipitation followed by Western blot analysis reveals a binding partner for Mcl-1 is NOXA and vice versa depending on the antibody used for either immunoprecipitation or Western blotting. Note when whole-cell lysates were immunoprecipitated with an anti-Mcl-1 antibody but not rabbit IgG, the bortezomib-treated melanoma cell immunoprecipitate for Mcl-1 also contained NOXA as detected by immunoblot analysis (*left*). Using a complementary approach in which anti-NOXA antibody, but not rabbit IgG, led to an immunoprecipitate that also contained Mcl-1 as detected by subsequent immunoblotting (*right*). For both approaches, the input analysis revealed that NOXA and Mcl-1 levels were increased in melanoma cells after bortezomib exposure. Actin levels confirm equivalent protein loading. Taken together, these results show binding between Mcl-1 and NOXA in bortezomib-treated melanoma cells.

Figure 2. Overexpression of Mcl-1 by retroviral infection reduces bortezomib-induced apoptosis ($1 \mu\text{mol/L}$; 24 hours) in RJ002L melanoma cells. **A**, Western blot analysis of Mcl-1 levels before and 24 hours after bortezomib exposure ($1 \mu\text{mol/L}$) in control (Linker) and Mcl-1-overexpressing melanoma cells. These results indicate a 2-fold increase in Mcl-1 levels by retroviral infection. Actin levels confirm equivalent protein loading. Whole-cell extracts and immunoblotting was done as described in Materials and Methods. **B**, quantitative assessment of apoptosis in RJ002L melanoma cells reveals no difference in spontaneous apoptosis but reduced apoptosis in Mcl-1-overexpressing melanoma cells. *, $P < 0.005$, significantly reduced killing of melanoma cells when Mcl-1 levels are increased and bortezomib is added to melanoma cells compared with control (Linker) infected cells. Cell death assessment was done by Annexin V/FACS analysis as described in Materials and Methods. *Columns*, mean of three independent experiments; *bars*, SE.



melanoma cells. Assessment of cell death using Annexin V/FACS analysis revealed no significant differences in the spontaneous apoptotic response to Mcl-1 siRNA exposure (10-11%), but the bortezomib-induced cell death ($1 \mu\text{mol/L}$; 24 hours) significantly increased from 25% in control siRNA-treated melanoma cells to 45% in Mcl-1 siRNA-treated melanoma cells (Fig. 3A). The Mcl-1 siRNA not only reduced constitutive Mcl-1 levels compared with control siRNA-treated cells, but the Mcl-1 siRNA also reduced bortezomib-induced accumulation of Mcl-1 (Fig. 3B). There was reduction in low constitutive NOXA levels by Mcl-1 siRNA and only a slight reduction in bortezomib-induced NOXA levels when comparing control siRNA with Mcl-1 siRNA-treated melanoma cells. The Mcl-1 siRNA treatment had no effects on constitutive or

bortezomib-treated levels of either Bcl-2 or Bcl- x_L . Protein levels of Bad, which were relatively high before bortezomib treatment, were reduced (but still detectable) in bortezomib-treated melanoma cells and not influenced by the Mcl-1 siRNA. Bortezomib treatment produced increased total cellular levels of Bak and decreased total Bax levels. Greater induction of cleaved PARP was apparent in bortezomib-exposed melanoma cells in the Mcl-1 siRNA-pretreated cells compared with control siRNA-treated melanoma cells. Taken together, the forced overexpression of Mcl-1, or the knockdown of Mcl-1, significantly influenced the bortezomib-induced death response of melanoma cells.

To further delineate the death machinery in melanoma cells, activated forms for both Bak and Bax were detected by FACS

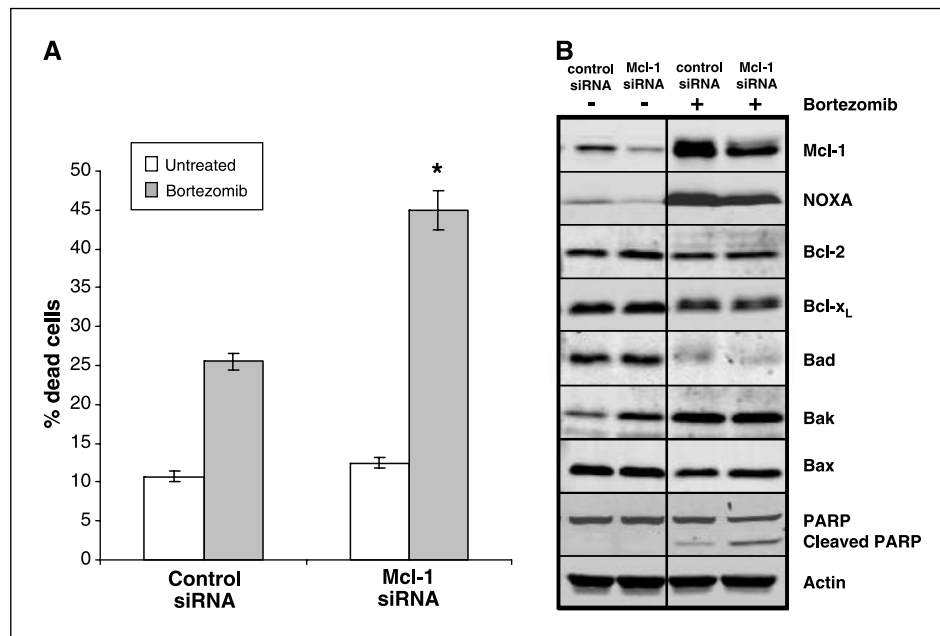


Figure 3. Knockdown of Mcl-1 levels using siRNA enhances bortezomib-induced cell death ($1 \mu\text{mol/L}$; 24 hours) of C8161 melanoma cells. **A**, quantitative assessment of cell death in C8161 melanoma cells reveals no difference in spontaneous levels between control siRNA and Mcl-1 siRNA treatment. However, Mcl-1 siRNA treatment followed by bortezomib exposure enhanced cell death compared with control siRNA-treated cells. *, $P < 0.005$, significantly enhanced killing of melanoma cells by bortezomib in Mcl-1 siRNA-treated cells compared with control siRNA-treated cells. Cell death assessment was done by Annexin V/FACS analysis as described in Materials and Methods. *Columns*, mean of three independent experiments; *bars*, SE. **B**, Western blot analysis of Mcl-1 levels before and after siRNA treatment reveals knockdown of constitutive levels as well as reduction in accumulation of Mcl-1 24 hours after bortezomib exposure ($1 \mu\text{mol/L}$). Mcl-1 siRNA treatment also slightly reduced constitutive NOXA levels and slightly increased Bak levels but did not significantly influence Bcl-2, Bcl- x_L , Bad, or PARP levels. In bortezomib-treated melanoma cells, the Bad levels were reduced in both control siRNA and Mcl-1 siRNA-treated cultures, with enhanced levels of cleaved PARP present in Mcl-1 siRNA-treated cells following bortezomib exposure. Actin levels confirm equivalent protein loading. Whole-cell extracts and immunoblotting was done as described in Materials and Methods.

analysis in both control siRNA and Mcl-1 siRNA-pretreated cells following bortezomib exposure (Fig. 4A). Although Bak and Bax in several experimental cell systems seem to be functionally equivalent in mediating cell death, and complete resistance is dependent on inactivation of both Bak and Bax (39), their activation by exposure of ordered NH₂-terminal sequences following bortezomib treatment of melanoma cells was examined. The antibodies used are well characterized and only recognize an epitope exposed when either Bak or Bax becomes activated (35, 36). In control siRNA-treated C8161 melanoma cells, no constitutive activated Bak or Bax levels are detected (Fig. 4A), and addition of bortezomib (1 $\mu\text{mol/L}$; 24 hours) only increased high levels of activated Bak (30.5%), with a less dramatic increase in activated Bak (5-7%). However, when Mcl-1 siRNA-treated melanoma cells were examined, addition of bortezomib (1 $\mu\text{mol/L}$; 24 hours) triggered prominent increase in both activated Bak (16.3%) and activated Bax (46.6%).

To confirm and extend these findings, subcellular localization profiles were done using MitoTracker Red CMXRos to identify intracellular mitochondria together with immunofluorescence staining to detect and localize activated Bax (Fig. 4B and C). When control siRNA-treated C8161 melanoma cells were examined

in the absence of bortezomib, there was no detection of activated Bax in the cells in either the mitochondrial compartment or elsewhere in the cytosol. Addition of bortezomib (1 $\mu\text{mol/L}$; 6 hours) revealed occasional melanoma cells with detectable activated Bax (green), which colocalized in the merged views with the red-labeled mitochondrial compartment (yellow; white arrows depicting double staining). When Mcl-1 siRNA-treated C8161 melanoma cells were examined, no detection of activated Bax was identified in the absence of bortezomib (Fig. 4C). However, with the addition of bortezomib (1 $\mu\text{mol/L}$; 6 hours), numerous melanoma cells expressing activated Bax (green), and the colocalization to the mitochondrial compartment (red) resulted in yellow stained cells when the images were merged (Fig. 4C, white arrows). Taken together, these results indicate the increased number of C8161 melanoma cells expressing activated Bak and Bax can be detected when bortezomib is added to the Mcl-1 siRNA-treated cells compared with control siRNA-treated cells. In the following sections, other approaches to reducing Mcl-1 levels were used (e.g., UV light or fludarabine), and the subsequent molecular and cellular efforts were defined following bortezomib exposure.

Modulation of Mcl-1 levels in melanoma cells following UV light exposure and bortezomib treatment. Because Mcl-1 is a

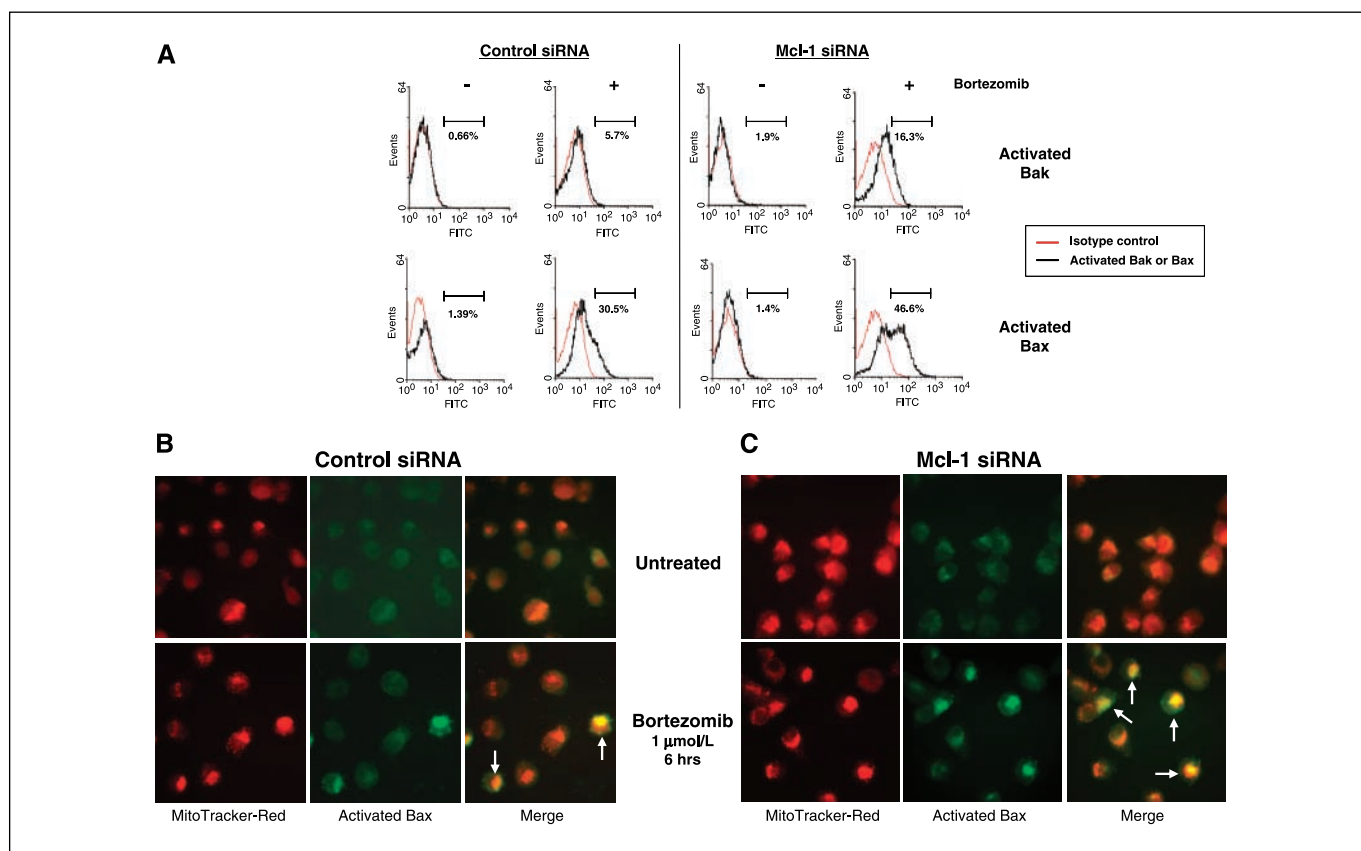


Figure 4. Knockdown of Mcl-1 levels with siRNA promotes bortezomib-induced Bak and Bax activation in C8161 melanoma cells. **A**, C8161 melanoma cells were transfected with control siRNA or Mcl-1 siRNA for 48 hours and then treated with 1 $\mu\text{mol/L}$ bortezomib for 24 hours. Intracellular staining for activated Bak and Bax was done as described in Materials and Methods. Representative flow cytometric profiles from three independent experiments reveal increased levels of Bak (*top*) and Bax (*bottom*) with activated conformation in the cells treated with Mcl-1 siRNA and bortezomib compared with the control siRNA and bortezomib-treated cells. The brackets and underlying percentages indicate the relative increase in cells expressing either activated Bak or Bax. **B** and **C**, C8161 melanoma cells transfected with control siRNA (**B**) and Mcl-1 siRNA (**C**) were treated with 1 $\mu\text{mol/L}$ bortezomib for 6 hours and labeled with MitoTracker Red CMXRos followed by immunofluorescence staining with anti-active form of Bax as described in Materials and Methods. The corresponding images of MitoTracker Red CMXRos (*red*) and activated Bax (*green*) were merged to show the colocalization of mitochondria and activated Bax (*white arrows*). In the untreated melanoma cells (no bortezomib), no activated Bax is identified within the mitochondrial compartment. Note the greater number of melanoma cells expressing activated Bax in the bortezomib-treated Mcl-1 siRNA cells compared with control siRNA cells.

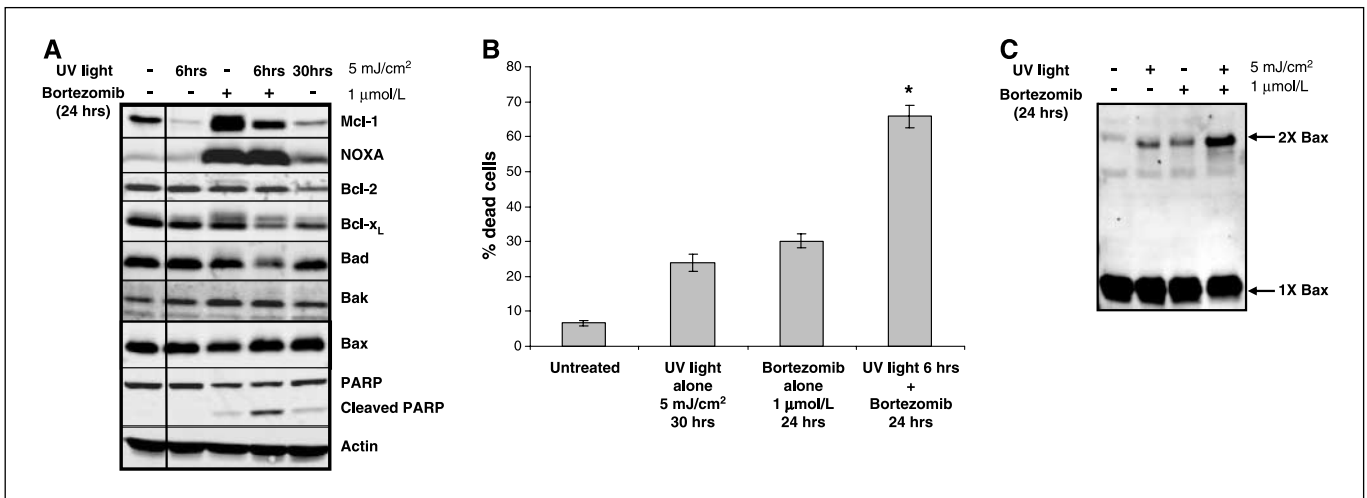


Figure 5. Pretreating C8161 melanoma cells with low-dose UV light reduces Mcl-1 levels and enhances bortezomib-induced cell death and Bax activation. *A*, Western blot analysis of whole-cell extracts before and after low-dose UV light (5 mJ/cm²) and/or bortezomib treatment reveals high constitutive levels of Mcl-1, Bcl-2, Bcl-x_L, Bad, Bak, and Bax with barely detectable NOXA and intact (noncleaved) PARP (*lane 1*). After 6 hours of UV light exposure, there is a reduction in Mcl-1 levels with no other significant changes in the other protein levels (*lane 2*). Twenty-four hours after bortezomib exposure (1 μmol/L), there is accumulation of Mcl-1 and induction of high NOXA levels with PARP cleavage (*lane 3*). When melanoma cells are pretreated with low-dose UV light and 6 hours later bortezomib is added, the following 24-hour incubation period is characterized by reduced accumulation of Mcl-1 and slightly lower Bad levels but high NOXA and cleaved PARP levels (*lane 4*). The relative protein levels 30 hours following low-dose UV light exposure revealed lower Mcl-1, Bcl-2, Bcl-x_L, and Bax levels compared with untreated cells with slight increase in NOXA levels and cleaved PARP (*lane 5*). Actin levels confirm equivalent protein loading. Whole-cell extracts and immunoblotting was done as described in Materials and Methods. *B*, quantitative assessment of cell death in C8161 melanoma cells reveals a low spontaneous level (7%), which is increased to 22% after 30 hours following a single low dose (5 mJ/cm²) of UV light. Bortezomib treatment alone (1 μmol/L; 24 hours) triggered 29% cell death response. A single low dose (5 mJ/cm²) of UV light followed 6 hours later by addition of bortezomib for an additional 24 hours increased the cell death response to 65%. *, *P* < 0.05, significantly enhanced killing of melanoma cells by a combination of single low dose (5 mJ/cm²) of UV light pretreatment followed by bortezomib compared with either agent used alone. Cell death assessment was done by Annexin V/FACS analysis as described in Materials and Methods. *Columns*, mean; *bars*, SE. *C*, C8161 melanoma cells were pretreated with UV light (5 mJ/cm²) for 6 hours and then treated with or without bortezomib for 24 hours followed by cross-linking with formaldehyde as described in Materials and Methods. The Western blot analysis with Bax antibody shows Bax monomer (1×) and Bax dimer (2×). Note the Bax dimer level significantly increased in cells treated with UV light + bortezomib.

short-lived protein normally degraded via the ubiquitin-proteasome pathway (29), addition of a proteasome inhibitor (e.g., bortezomib) leads to accumulation of Mcl-1 (11–13). In other systems, reduction or loss of Mcl-1 is required for optimal apoptotic responses, and UV irradiation has been described previously as potent method to modulate Mcl-1 levels (30, 40). To determine the effect of UV light alone and in combination with bortezomib, C8161 melanoma cells were examined before and after treatment and analyzed for relative levels of important proteins regulating apoptosis as well as the extent of cell death under each experimental condition. C8161 melanoma cells are characterized by high constitutive levels of several prosurvival proteins, including Mcl-1, Bcl-2, and Bcl-x_L, as well as proapoptotic Bad and Bax, but only relatively low Bak and even lower NOXA levels (Fig. 5A). A single low dose of UV light (5 mJ/cm²) reduces Mcl-1 levels as early as 1 hour after irradiation and was 4-fold lower after 6 hours of irradiation. The reduced Mcl-1 levels were sustained 30 hours after UV light exposure with no comparable effects on the other protein levels (compare *lanes 2* and *5* with *lane 1*). Exposure to bortezomib alone leads to accumulation of Mcl-1 levels (*lane 3*), and the pretreatment with UV light for 6 hours reduces the bortezomib-induced Mcl-1 levels (compare *lane 4* with *lane 3*) after a subsequent 24-hour exposure interval to bortezomib (1 μmol/L) without affecting other protein levels, except for Bad, which was decreased 30 hours after a single dose of UV light and also reduced by bortezomib alone or UV light plus bortezomib. UV light irradiation alone did not induce NOXA after 6 hours and only slightly increased NOXA levels after 30 hours. When melanoma cells were pretreated with UV light for 6 hours and then exposed to bortezomib for 24 hours (*lane 4*),

the high NOXA levels and lowered Mcl-1 levels were associated with higher levels of cleaved PARP.

Quantitative analysis of cell death was accomplished by Annexin V/FACS analysis using C8161 melanoma cells before and after the aforementioned single and combination treatments (Fig. 5B). A single exposure to UV light (5 mJ/cm²) produced a 22% cell death response after 30 hours compared with untreated cells (7%). Bortezomib alone (1 μmol/L) triggered a cell death response of 29% after 24 hours. Preirradiating C8161 melanoma cells for 6 hours followed by an additional 24 hours of bortezomib exposure triggered significant enhancement of cell death reaching 65% of the total cell population. Following up on the previous results using FACS and immunofluorescence-based cell staining to detect activated Bax, an additional biochemical approach was used that involved detection of Bax dimers by Western blot analysis. Activation of Bax can be detected by cross-linking intracellular proteins as described previously (38), and Fig. 5C revealed the presence of Bax dimers in C8161 melanoma cells after UV light or bortezomib treatment. Furthermore, when both UV light and bortezomib are combined, an increased level of Bax dimer can be detected compared with the individual treatments.

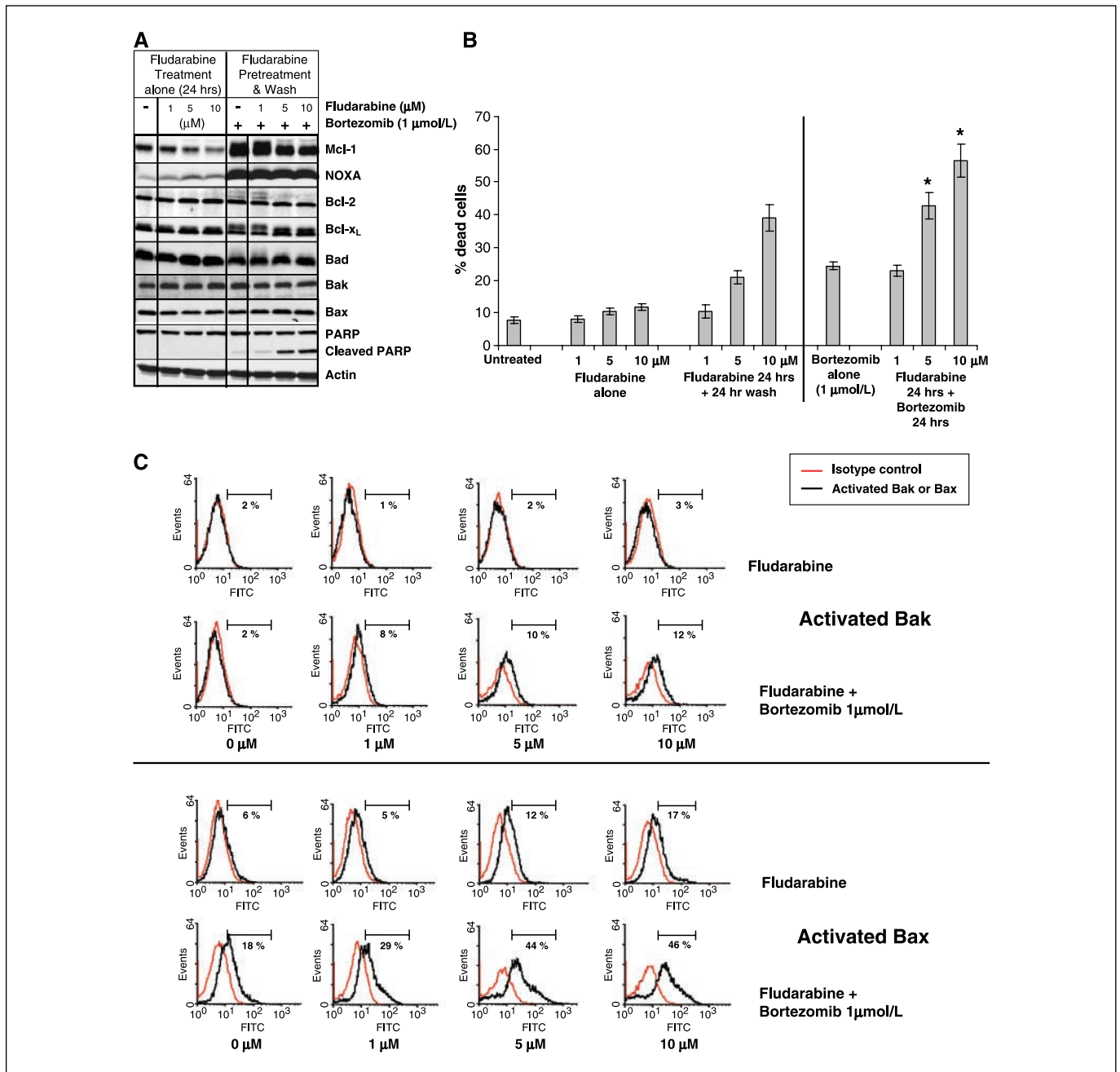
Based on these results, it seemed that the apoptotic response of melanoma cells to bortezomib included a pathway involving Mcl-1; therefore, additional experiments were designed to exploit this observation from a therapeutic perspective by combining bortezomib with a pretreatment protocol taking advantage of the ability of fludarabine to reduce Mcl-1 levels.

Combination of fludarabine and bortezomib enhances apoptotic response of melanoma cell killing. To further define

the relative role for Mcl-1 levels in the bortezomib-mediated apoptotic response of melanoma cells, a therapeutically relevant strategy was employed using fludarabine. Fludarabine was selected for this drug combination approach because of its ability to reduce Mcl-1 levels (31), and other groups have reported enhanced killing of tumor cells by targeting Mcl-1 using other agents (41, 42). A dose-dependent (1, 5, and 10 $\mu\text{mol/L}$) reduction in high constitutive Mcl-1 levels was observed at 24 hours in C8161 melanoma cells following exposure to fludarabine alone, with no significant effect on levels of other Bcl-2 family members, such as Bcl-2, Bcl-x_L, and Bad (Fig. 6A). Fludarabine treatment alone over the dose range used in this experimental setting for 24 hours had minimal effect on NOXA levels and no effect on total cellular levels of Bak, Bax, or PARP levels. C8161 melanoma cells

pretreated with increasing concentrations of fludarabine for 24 hours followed by washing and then exposed to bortezomib produced a dose-dependent reduction in the accumulation of Mcl-1 with minimal effects on Bcl-2, Bcl-x_L, Bak, and Bax (Fig. 6A). Whereas the pretreatment with fludarabine did not influence bortezomib-induced NOXA levels or Bcl-2 and Bcl-x_L levels, there was an overall reduction in Bad levels in cells exposed to bortezomib. The pretreatment with fludarabine followed by bortezomib was also associated with a dose-dependent increase in cleaved PARP levels, being greatest at the two highest fludarabine doses.

Compared with spontaneous levels of C8161 melanoma cell death (untreated; 8% by Annexin V/FACS analysis), there was no significant induction in cell death after 24 hours by fludarabine



when used alone (1, 5, and 10 $\mu\text{mol/L}$; 9-11% by Annexin V/FACS analysis; Fig. 6B). The cell death response in C8161 melanoma cells exposed to increasing concentrations of fludarabine alone for 24 hours followed by washing and an additional 24 hours revealed increased cell death at the 5 and 10 $\mu\text{mol/L}$ doses (21% and 39%, respectively). When bortezomib (1 $\mu\text{mol/L}$) was added as a single agent, the 24-hour cell death response was 24%. Although pretreating C8161 melanoma cells with 1 $\mu\text{mol/L}$ fludarabine for 24 hours and then washing and adding bortezomib for an additional 24 hours did not increase the cell death response (23%), when the fludarabine pretreatment concentration was increased to 5 and 10 $\mu\text{mol/L}$, addition of bortezomib increased the cell death response to 43% and 57%, respectively. These increased death responses were consistent with the increased PARP levels as depicted in Fig. 6A.

To further characterize the response of melanoma cells to the combination of fludarabine pretreatment followed by bortezomib exposure, the relative levels of activated Bak and Bax were examined using FACS analysis. Exposure to fludarabine alone (24 hours; 1, 5, and 10 $\mu\text{mol/L}$) triggered no increase in activated Bak levels but increased the activated Bax levels at the 5 and 10 $\mu\text{mol/L}$ concentrations from 6% in untreated cells to 12% and 17%, respectively (Fig. 6C). When C8161 melanoma cells were treated with fludarabine at the indicated concentrations for 24 hours, washed, and then exposed to bortezomib (1 $\mu\text{mol/L}$) for an additional 24 hours, activated Bak levels increased from 2% to 8%, 10%, and 12% at the 1, 5, and 10 $\mu\text{mol/L}$ fludarabine concentrations, respectively (Fig. 6C, top). When C8161 melanoma cells were treated with fludarabine at the indicated concentrations for 24 hours, washed, and then exposed to bortezomib (1 $\mu\text{mol/L}$) for an additional 24 hours, activated Bax levels increased from 18% to 29%, 44%, and 46% at the 1, 5, and 10 $\mu\text{mol/L}$ fludarabine concentrations, respectively (Fig. 6C, bottom). Taken together, these results indicate that pretreatment of melanoma cells with fludarabine followed by bortezomib exposure enhances intracellular levels of activated conformations of both Bak and Bax.

A summary of the working model by which a combination of fludarabine and bortezomib produce enhanced melanoma cell

killing, in which NOXA, Mcl-1, and activated Bak and Bax are highlighted, is provided in Fig. 7.

Discussion

Targeting the proteasome function has turned out to be an excellent antireplicative strategy for oncologists in a variety of clinical settings (43). The 26S proteasome is composed of a multicatalytic protease functioning to regulate a larger number of intracellular protein levels. Various inhibitors can reversibly block the chymotryptic-like proteolytic activity of the proteasome complex (14). Of particular note is the relative sparing by proteasome inhibitors of normal, nonmalignant cells from apoptosis but also the ability to bypass classic multidrug resistance mechanisms (44).

Precise molecular details controlling cell death decisions are rapidly emerging from several laboratories (45-47). As regards the multidomain-mediated apoptotic pathway, a distinctive mode of regulation has been proposed by which proapoptotic proteins, such as Bak and Bax, are normally prevented from activation by direct sequestration due to two different prosurvival proteins, Mcl-1 and Bcl-x_L (24, 25). The conformational change associated with Bak and Bax toxicity when Mcl-1 and Bcl-x_L are displaced by NOXA and Bad, respectively, can be quantitated using antibodies directed against a NH₂-terminal epitope in Bak and Bax (35). To determine if this model could be exploited therapeutically, we defined the molecular machinery engaged by a proteasome inhibitor in melanoma cells. Moreover, the relative roles for NOXA/Mcl-1 versus Bad/Bcl-x_L could be assessed in melanoma cells. Indeed, this model was validated and successfully exploited because we showed that NOXA bound to Mcl-1 and by simultaneously inducing NOXA and reducing Mcl-1 levels, leading to enhanced levels of activated Bak and Bax accompanied by killing of melanoma cells. A summary of our current working model for these molecular mechanistic pathway by which a combination of bortezomib plus fludarabine produced enhanced killing of melanoma cells is presented in Fig. 7.

The accumulation of the prosurvival protein Mcl-1 is not surprising following bortezomib exposure, given that the proteasome

Figure 6. Enhanced C8161 melanoma cell killing by pretreating with fludarabine followed by bortezomib. **A**, Western blot analysis of whole-cell extracts before and after increasing concentrations of fludarabine and/or bortezomib treatment reveals high constitutive levels of Mcl-1, Bcl-2, Bcl-x_L, Bad, Bak, and Bax with barely detectable NOXA and intact (noncleaved) PARP (lane 1). After 24 hours of fludarabine exposure, there is a reduction in Mcl-1 levels with no other significant changes in the other protein levels, except for slight induction of NOXA levels (lanes 2-4). Twenty-four hours after bortezomib exposure (1 $\mu\text{mol/L}$), there is accumulation of Mcl-1 and induction of high NOXA levels with ubiquitinated forms of Bcl-2, with lower Bad and higher Bak levels compared with untreated cells, accompanied by PARP cleavage (lane 5). When melanoma cells are pretreated with increasing doses of fludarabine for 24 hours and washed and then bortezomib is added, the following 24-hour incubation period is characterized by reduced accumulation of Mcl-1 but high NOXA and particularly high levels of cleaved PARP detected at the 5 and 10 $\mu\text{mol/L}$ doses of fludarabine (lanes 6-8). Actin levels confirm equivalent protein loading. Whole-cell extracts and immunoblotting was done as described in Materials and Methods. **B**, quantitative assessment of cell death in C8161 melanoma cells reveals a low spontaneous level (8%), which is not significantly increased by 24-hour exposure to fludarabine alone (1, 5, and 10 $\mu\text{mol/L}$). When fludarabine is used alone for 24 hours, and the cells are washed and examined after an additional 24 hours, there is a dose-dependent increase in cell death at the 5 $\mu\text{mol/L}$ (24%) and 10 $\mu\text{mol/L}$ (39%) concentrations. Bortezomib treatment alone (1 $\mu\text{mol/L}$; 24 hours) triggered 24% cell death response. When fludarabine was added for 24 hours, and the cells were washed and then exposed to bortezomib for an additional 24 hours, although there was no increased cell death at the concentration of 1 $\mu\text{mol/L}$ fludarabine, the use of fludarabine at 5 and 10 $\mu\text{mol/L}$ did increase the cell death response (43% and 57%, respectively). *, $P < 0.01$, significantly enhanced killing of melanoma cells by a combination of fludarabine pretreatment at 5 and 10 $\mu\text{mol/L}$ doses followed by bortezomib compared with either agent used alone. Cell death assessment was done by Annexin V/FACS analysis as described in Materials and Methods. **Columns**, mean; **bars**, SE. **C**, response of C8161 melanoma cells to fludarabine (1, 5, and 10 $\mu\text{mol/L}$) and/or bortezomib (1 $\mu\text{mol/L}$) reveals altered intracellular levels of activated Bak and activated Bax. Compared with low constitutive activated Bak or Bax levels (2% and 6%, respectively), the cell death response to fludarabine alone at all concentrations after 24 hours is characterized by no to minimal increases in intracellular levels of activated Bak, whereas activated Bax is increased at 5 and 10 $\mu\text{mol/L}$ to 12% and 17%, respectively. Pretreatment of C8161 melanoma cells with fludarabine (24 hours) followed by washing and exposure to bortezomib (24 hours) triggered enhanced activated Bak levels at 1, 5, and 10 $\mu\text{mol/L}$ concentrations of fludarabine of 8%, 10%, and 12%, respectively. Pretreatment of C8161 melanoma cells with fludarabine (24 hours) followed by washing and exposure to bortezomib (24 hours) triggered enhanced activated Bax levels at 1, 5, and 10 $\mu\text{mol/L}$ concentrations of fludarabine of 29%, 44%, and 46%, respectively. Taken together, these results show that pretreatment with fludarabine followed by bortezomib triggers conformational changes leading to activation of both Bak and Bax in melanoma cells. Quantitation of melanoma cells expressing activated Bak or Bax was done using FACS and setting the gates based on isotype control antibody staining profiles versus staining intensity detected by using antibodies specific for activated conformations of Bak and Bax as described in Materials and Methods. The bars and the underlying percentages indicate the relative increase in cells expressing either activated Bak or Bax.

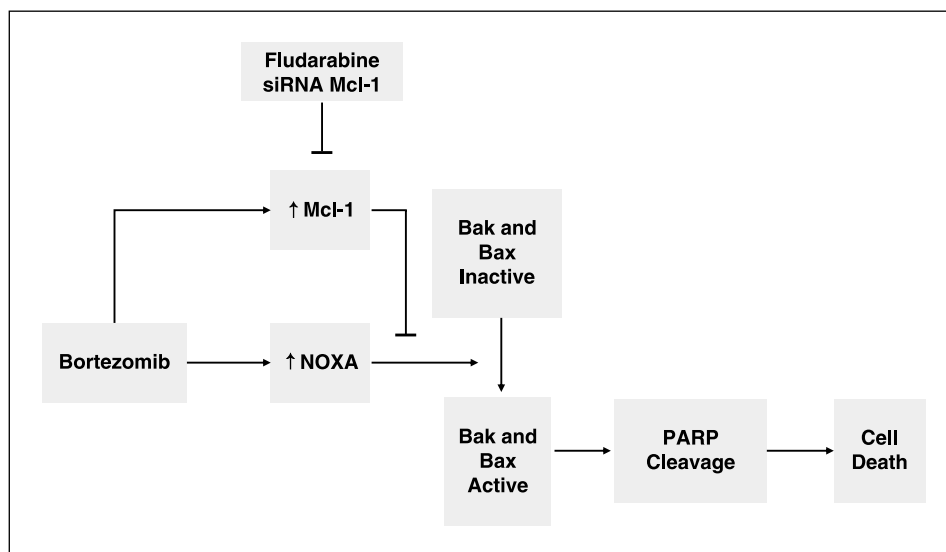


Figure 7. Model for apoptotic pathway by which a combination of bortezomib + fludarabine produces enhanced conversion of inactive to active conformation of Bak and Bax accompanied by increased PARP cleavage and killing of melanoma cells. The key elements of this model include a strategy by which inhibition of proteasome activity (via bortezomib) not only triggers proapoptotic NOXA induction but also counteracts the undesirable accumulation of antiapoptotic Mcl-1 levels (using siRNA against Mcl-1 or using fludarabine pretreatment).

mediates the degradation of many proteins involved in cellular proliferation and apoptosis. Thus, to increase the effectiveness of killing by bortezomib, it is important to consider adding a second agent that can interfere with the Mcl-1 accumulation. By pretreating melanoma cells with either Mcl-1 siRNA, low-dose UV light, or fludarabine, Mcl-1 levels were reduced sufficiently to enhance the effectiveness of NOXA accompanied by increased melanoma cell death. Another set of important observations was the relatively low levels of Bad present in bortezomib-treated melanoma cells (Figs. 5 and 6), suggesting a greater role for NOXA in displacing Mcl-1, compared with Bad displacing Bcl-x_L, in this neoplastic system using a proteasome inhibitor. These results provide a molecular basis for rational combination therapies operating through the mitochondrial apoptotic pathway in which bortezomib is used together with other agents targeting Mcl-1 (48).

Using proteasome inhibitors with melanoma cells has provided new insights not only into the apoptotic resistance of these aggressive tumor cells but also into new pathways that can be designed to overcome the apoptotic resistance of melanoma while sparing normal melanocytes (43). Exposing melanoma cells to conventional chemotherapeutic agents have yielded only modest proapoptotic responses, and several antiapoptotic factors have been invoked to explain this relative refractoriness. The best single agent activating against melanoma is dacarbazine or its derivative temozolomide, but only a 10% to 15% response rate is observed with a 4-month median response duration (49). Specific mechanisms by which melanoma cells acquire their notorious resistance to either extrinsic or intrinsic pathway-mediated killing include activation of Ras with increased levels of Bcl-2 (50, 51), increased survivin levels (52), loss of death receptors (53, 54), and reduction in Apaf-1 expression (55–57).

To overcome this apoptotic resistance, we and others have discovered a key role for the proapoptotic BH3-only protein NOXA, which is selectively induced by proteasome inhibitors (in a p53-independent fashion) but not conventional chemotherapeutic agents, such as Adriamycin or etoposide (11–13, 58). Of perhaps equal importance is the sparing of NOXA induction or killing of normal melanocytes by bortezomib (11–13, 58). Given the disappointing phase II clinical trial results using bortezomib as a

single agent (18), we decided to further interrogate the apoptotic machinery engaged within melanoma cells that were exposed to bortezomib to determine a rational basis for selecting an appropriate agent to combine with bortezomib and hence potentially improve the killing of melanoma cells. The clear-cut binding partnership established between NOXA and Mcl-1 paved the pathway to the studies herein focused on Mcl-1. As revealed in this report, the use of several different mediators to modulate Mcl-1 influenced the apoptotic susceptibility in melanoma cells exposed to bortezomib, validating the approach for a rational drug combination therapy.

For practical considerations, we selected fludarabine as an appropriate pharmacologic agent to combine with bortezomib given the ability of fludarabine to reduce Mcl-1 levels that became elevated and thereby counteract the proapoptotic effects of NOXA induction by bortezomib. Another group observed synergistic killing of leukemia cells when either fludarabine or another purine nucleoside analogue, cladribine, was combined with bortezomib (33). By combining bortezomib with fludarabine, not only is it likely that a greater and more durable clinical effect as regards killing of melanoma cells can be achieved, but also it may also be possible to use lower drug concentrations and avoid or minimize toxicities that can limit the usefulness of either drug administered individually in patients with melanoma. In conclusion, the current results support further studies, including a clinical trial in which patients with metastatic melanoma are treated with a combination of bortezomib plus fludarabine, and tissue samples were examined to assess the relative levels of NOXA and Mcl-1 within tumor cells before and after this combination therapy in responders and nonresponders.

Acknowledgments

Received 2/27/2006; revised 5/26/2006; accepted 7/19/2006.

Grant support: NIH grants CA 59327, CA 27502 (B.J. Nickoloff), and CA083784 (M.F. Denning).

The costs of publication of this article were defrayed in part by the payment of page charges. This article must therefore be hereby marked *advertisement* in accordance with 18 U.S.C. Section 1734 solely to indicate this fact.

We thank Lynn Walter for expert figure and article preparation and Jeffrey Ziffra, Barbara Bodner, and Larry Stennett for expert technical assistance.

References

1. Jemal A, Thomas A, Murray T, Thun M. Cancer statistics, 2002. *CA Cancer J Clin* 2002;52:23–47.
2. Soengas MS, Lowe SW. Apoptosis and melanoma chemoresistance. *Oncogene* 2003;22:3138–51.
3. Chang AE, Karnell LH, Menck HR. The National Cancer Data Base report on cutaneous and noncutaneous melanoma: a summary of 84,836 cases from the past decade. The American College of Surgeons Commission on Cancer and the American Cancer Society. *Cancer* 1998;83:1664–78.
4. Grossman D, Kim PJ, Schechner JS, Altieri DC. Inhibition of melanoma tumor growth *in vivo* by survivin targeting. *Proc Natl Acad Sci U S A* 2001;98:635–40.
5. Helmbach H, Rossmann E, Kern MA, Schadendorf D. Drug-resistance in human melanoma. *Int J Cancer* 2001;93:617–22.
6. Mandara M, Nortilli R, Sava T, Cetto GL. Chemotherapy for metastatic melanoma. *Expert Rev Anticancer Ther* 2006;6:121–30.
7. Chin L, Merlino G, DePinho RA. Malignant melanoma: modern black plague and genetic black box. *Genes Dev* 1998;12:3467–81.
8. Grossman D, Altieri DC. Drug resistance in melanoma: mechanisms, apoptosis, and new potential therapeutic targets. *Cancer Metastasis Rev* 2001;20:3–11.
9. Hussein MR, Haemel AK, Wood GS. Apoptosis and melanoma: molecular mechanisms. *J Pathol* 2003;199:275–88.
10. Tron VA, Krajewski S, Klein-Parker H, et al. Immunohistochemical analysis of Bcl-2 protein regulation in cutaneous melanoma. *Am J Pathol* 1995;146:643–50.
11. Fernandez Y, Verhaegen M, Miller TP, et al. Differential regulation of noxa in normal melanocytes and melanoma cells by proteasome inhibition: therapeutic implications. *Cancer Res* 2005;65:6294–304.
12. Qin JZ, Stennett L, Bacon P, et al. p53-independent NOXA induction overcomes apoptotic resistance of malignant melanomas. *Mol Cancer Ther* 2004;3:895–902.
13. Qin JZ, Ziffra J, Stennett L, et al. Proteasome inhibitors trigger NOXA-mediated apoptosis in melanoma and myeloma cells. *Cancer Res* 2005;65:6282–93.
14. Dalton WS. The proteasome. *Semin Oncol* 2004;31:3–9.
15. Satyamoorthy K, Bogenrieder T, Herlyn M. No longer a molecular black box—new clues to apoptosis and drug resistance in melanoma. *Trends Mol Med* 2001;7:191–4.
16. Chudnovsky Y, Khavari PA, Adams AE. Melanoma genetics and the development of rational therapeutics. *J Clin Invest* 2005;115:813–24.
17. Amiri KI, Horton LW, LaFleur BJ, Sosman JA, Richmond A. Augmenting chemosensitivity of malignant melanoma tumors via proteasome inhibition: implication for bortezomib (Velcade, PS-341) as a therapeutic agent for malignant melanoma. *Cancer Res* 2004;64:4912–8.
18. Markovic SN, Geyer SM, Dawkins F, et al. A phase II study of bortezomib in the treatment of metastatic malignant melanoma. *Cancer* 2005;103:2584–9.
19. Green DR, Kroemer G. The pathophysiology of mitochondrial cell death. *Science* 2004;305:626–9.
20. Huang DC, Strasser A. BH3-only proteins—essential initiators of apoptotic cell death. *Cell* 2000;103:839–42.
21. Strasser A. The role of BH3-only proteins in the immune system. *Nat Rev Immunol* 2005;5:189–200.
22. Gelinas C, White E. BH3-only proteins in control: specificity regulates MCL-1 and BAK-mediated apoptosis. *Genes Dev* 2005;19:1263–8.
23. Lindsten T, Ross AJ, King A, et al. The combined functions of proapoptotic Bcl-2 family members bak and bax are essential for normal development of multiple tissues. *Mol Cell* 2000;6:1389–99.
24. Chen L, Willis SN, Wei A, et al. Differential targeting of prosurvival Bcl-2 proteins by their BH3-only ligands allows complementary apoptotic function. *Mol Cell* 2005;17:393–403.
25. Willis SN, Chen L, Dewson G, et al. Proapoptotic Bak is sequestered by Mcl-1 and Bcl-xL, but not Bcl-2, until displaced by BH3-only proteins. *Genes Dev* 2005;19:1294–305.
26. Lang-Rollin I, Maniati M, Jabado O, et al. Apoptosis and the conformational change of Bax induced by proteasomal inhibition of PC12 cells are inhibited by bcl-xL and bcl-2. *Apoptosis* 2005;10:809–20.
27. Panaretakis T, Pokrovskaja K, Shoshan MC, Grandeur D. Activation of Bak, Bax, and BH3-only proteins in the apoptotic response to doxorubicin. *J Biol Chem* 2002;277:44317–26.
28. von Haefen C, Gillissen B, Hemmati PG, et al. Multidomain Bcl-2 homolog Bax but not Bak mediates synergistic induction of apoptosis by TRAIL and 5-FU through the mitochondrial apoptosis pathway. *Oncogene* 2004;23:8320–32.
29. Iglesias-Serret D, Pique M, Gil J, Pons G, Lopez JM. Transcriptional and translational control of Mcl-1 during apoptosis. *Arch Biochem Biophys* 2003;417:141–52.
30. Chaturvedi V, Sitailo LA, Qin JZ, et al. Knockdown of p53 levels in human keratinocytes accelerates Mcl-1 and Bcl-x(L) reduction thereby enhancing UV-light induced apoptosis. *Oncogene* 2005;24:5299–312.
31. Maggio SC, Rosato RR, Kramer LB, et al. The histone deacetylase inhibitor MS-275 interacts synergistically with fludarabine to induce apoptosis in human leukemia cells. *Cancer Res* 2004;64:2590–600.
32. Robak T, Korycka A, Kasznicki M, Wrzesien-Kus A, Smolewski P. Purine nucleoside analogues for the treatment of hematological malignancies: pharmacology and clinical applications. *Curr Cancer Drug Targets* 2005;5:421–44.
33. Duechler M, Linke A, Cebula B, et al. *In vitro* cytotoxic effect of proteasome inhibitor bortezomib in combination with purine nucleoside analogues on chronic lymphocytic leukaemia cells. *Eur J Haematol* 2005;74:407–17.
34. Armstrong JS. Mitochondria: a target for cancer therapy. *Br J Pharmacol* 2005;147:239–48.
35. Griffiths GJ, Dubrez L, Morgan CP, et al. Cell damage-induced conformational changes of the pro-apoptotic protein Bak *in vivo* precede the onset of apoptosis. *J Cell Biol* 1999;144:903–14.
36. Nechushtan A, Smith CL, Hsu YT, Youle RJ. Conformation of the Bax C-terminus regulates subcellular location and cell death. *EMBO J* 1999;18:2330–41.
37. Qin JZ, Bacon P, Panella J, et al. Low-dose UV-radiation sensitizes keratinocytes to TRAIL-induced apoptosis. *J Cell Physiol* 2004;200:155–66.
38. Sitailo LA, Tibudan SS, Denning MF. Bax activation and induction of apoptosis in human keratinocytes by the protein kinase C δ catalytic domain. *J Invest Dermatol* 2004;123:434–43.
39. Wei MC, Zong WX, Cheng EH, et al. Proapoptotic BAX and BAK: a requisite gateway to mitochondrial dysfunction and death. *Science* 2001;292:727–30.
40. Nijhawan D, Fang M, Traer E, et al. Elimination of Mcl-1 is required for the initiation of apoptosis following ultraviolet irradiation. *Genes Dev* 2003;17:1475–86.
41. Battle TE, Arbiser J, Frank DA. The natural product honokiol induces caspase-dependent apoptosis in B-cell chronic lymphocytic leukemia (B-CLL) cells. *Blood* 2005;106:690–7.
42. Ma Y, Cress WD, Haura EB. Flavopiridol-induced apoptosis is mediated through up-regulation of E2F1 and repression of Mcl-1. *Mol Cancer Ther* 2003;2:73–81.
43. Adams J. The proteasome: a suitable antineoplastic target. *Nat Rev Cancer* 2004;4:349–60.
44. Dalton W. Drug resistance in hematologic malignancies. *Clin Adv Hematol Oncol* 2005;3:267–8.
45. Daniai NN, Korsmeyer SJ. Cell death: critical control points. *Cell* 2004;116:205–19.
46. Reed JC. Apoptosis-targeted therapies for cancer. *Cancer Cell* 2003;3:17–22.
47. Strasser A, O'Connor L, Dixit VM. Apoptosis signaling. *Annu Rev Biochem* 2000;69:217–45.
48. Shore GC, Viallet J. Modulating the bcl-2 family of apoptosis suppressors for potential therapeutic benefit in cancer. *Am Soc Hematol Educ Program* 2005;226–30.
49. Sun W, Schuchter LM. Metastatic melanoma. *Curr Treat Options Oncol* 2001;2:193–202.
50. Borner C, Schlagbauer Wadl H, Fellay I, et al. Mutated N-ras upregulates Bcl-2 in human melanoma *in vitro* and in SCID mice. *Melanoma Res* 1999;9:347–50.
51. Davies H, Bignell GR, Cox C, et al. Mutations of the BRAF gene in human cancer. *Nature* 2002;417:949–54.
52. Grossman D, McNiff JM, Li F, Altieri DC. Expression and targeting of the apoptosis inhibitor, survivin, in human melanoma. *J Invest Dermatol* 1999;113:1076–81.
53. Hersey P, Zhang XD. How melanoma cells evade trail-induced apoptosis. *Nat Rev Cancer* 2001;1:142–50.
54. Ivanov VN, Bhoumik A, Ronai Z. Death receptors and melanoma resistance to apoptosis. *Oncogene* 2003;22:3152–61.
55. Allen JD, Zhang XD, Scott CL, et al. Is Apaf-1 expression frequently abrogated in melanoma? *Cell Death Differ* 2005;12:680–1.
56. Peltenburg LT, de Bruin EC, Meersma D, et al. Expression and function of the apoptosis effector Apaf-1 in melanoma. *Cell Death Differ* 2005;12:678–9.
57. Soengas MS, Capodici P, Polsky D, et al. Inactivation of the apoptosis effector Apaf-1 in malignant melanoma. *Nature* 2001;409:207–11.
58. Fernandez Y, Miller TP, Denoyelle C, et al. Chemical blockage of the proteasome inhibitory function of bortezomib: impact on tumor cell death. *J Biol Chem* 2006;281:1107–18.

Cancer Research

The Journal of Cancer Research (1916–1930) | The American Journal of Cancer (1931–1940)

Enhanced Killing of Melanoma Cells by Simultaneously Targeting Mcl-1 and NOXA

Jian-Zhong Qin, Hong Xin, Leonid A. Sitailo, et al.

Cancer Res 2006;66:9636-9645.

Updated version Access the most recent version of this article at:
<http://cancerres.aacrjournals.org/content/66/19/9636>

Cited articles This article cites 57 articles, 18 of which you can access for free at:
<http://cancerres.aacrjournals.org/content/66/19/9636.full#ref-list-1>

Citing articles This article has been cited by 21 HighWire-hosted articles. Access the articles at:
<http://cancerres.aacrjournals.org/content/66/19/9636.full#related-urls>

E-mail alerts [Sign up to receive free email-alerts](#) related to this article or journal.

Reprints and Subscriptions To order reprints of this article or to subscribe to the journal, contact the AACR Publications Department at pubs@aacr.org.

Permissions To request permission to re-use all or part of this article, use this link
<http://cancerres.aacrjournals.org/content/66/19/9636>.
Click on "Request Permissions" which will take you to the Copyright Clearance Center's (CCC) Rightslink site.